(19), for the trapped-particle and flute limits of the perturbation, respectively.

[1]I. B. Bernstein, E. A. Frieman, M. D. Kruskal, and R. M. Kulsrud, Proc. Roy. Soc., Ser. A 244, 17 (1958).
[2]M. N. Rosenbluth and N. Rostoker, Phys. Fluids 2, 23 (1959).
[3]M. D. Kruskal and C. R. Oberman, Phys. Fluids 1, 275 (1958).
[4]C. Mercier, Nucl. Fusion 1, 47 (1960).
[5]V. D. Shafranov, in *Reviews of Plasma Physics*, edited by M. A. Leontovich (Consultants Bureau, New York, 1965), Vol. 2, p. 103.
[6]A. A. Ware and F. A. Haas, Phys. Fluids 9, 956 (1966).
[7]J. M. Greene, J. L. Johnson, and K. E. Weimer, Phys. Fluids 14, 671 (1971).
[8]V. D. Shafranov and E. I. Yurchenko, Zh. Eksp. Teor. Fiz. 53, 1157 (1967) [Sov. Phys. JETP 26, 682 (1968)].
[9]L. S. Soloviev, Zh. Eksp. Teor. Fiz. 53, 626 (1968) [Sov. Phys. JETP 26, 400 (1968)].
[10]R. M. Kulsrud, Phys. Fluids 5, 192 (1962).
[11]H. Grad, Phys. Fluids 9, 225 (1966).
[12]M. N. Rosenbluth, Phys. Fluids 11, 869 (1968).

Ablation Stability of Laser-Driven Implosions*

D. B. Henderson, R. L. McCrory, and R. L. Morse
University of California, Los Alamos Scientific Laboratory, Los Alamos, New Mexico 87544
(Received 29 April 1974)

Perturbation analysis of the stability of ablative, laser-driven implosions of homogeneous spherical pellets shows stability of the ablation surface, a necessary condition for achieving the high densities required for laser fusion. This conclusion is supported by physical arguments.

Recent interest in laser-driven implosion of spherical pellets of thermonuclear fuel to high densities has raised questions about the possibility of maintaining sufficient symmetry in such implosions to achieve the desired high densities. The problem has two complementary parts which are similar in their role and relationship to one another as are the equilibrium and stability of magnetic confinement of plasma. First, the flow of heat to the ablation surface of an implosion system must have sufficient spherical symmetry that the implosion can be approximately spherical; i.e., that asymmetries are not forced to occur by asymmetry of the external-laser-energy deposition and flow. Second, the ablation surface itself must be stable, a subject about which there is disagreement. Instability of this surface would almost certainly preclude success of laser fusion. In fact some positive stability may be required to compensate for small heat-input asymmetries. That these two problems are different and distinct becomes especially clear when one considers implosion systems in which the thermally conducting plasma cloud outside of the ablation surface is highly asymmetrical.

It has been observed by Henderson and Morse[1] that small departures from spherical symmetry of the coupled hydrodynamic and heat-flow processes involved can be analyzed by a linear perturbation expansion in scalar spherical harmonics $Y_l^m(\bar{\Omega})$, and that the analysis is greatly simplified by a decoupling of equations for different l's and a degeneracy with respect to the m's. This technique has been applied to the symmetry problem, by the use of stationary zero-order densities and temperatures, and criteria for acceptable symmetry of laser illumination have been developed.[2] Here we present calculations done with a combined zero- and first-order computer code developed specifically for the purpose of studying the stability problem with self-consistent, time-dependent zero-order densities and temperatures. This code is entirely distinct from that used in Ref. 2. These calculations show positive stability of the ablation surface during the implosion of homogeneous, spherical DT pellets. Physical arguments are presented which support our conclusion. Shiau, Goldman, and Weng,[3] using the same perturbation-expansion technique but not the identical numerical method, have reached the opposite conclusion.

The zero-order spherical-implosion case cho-

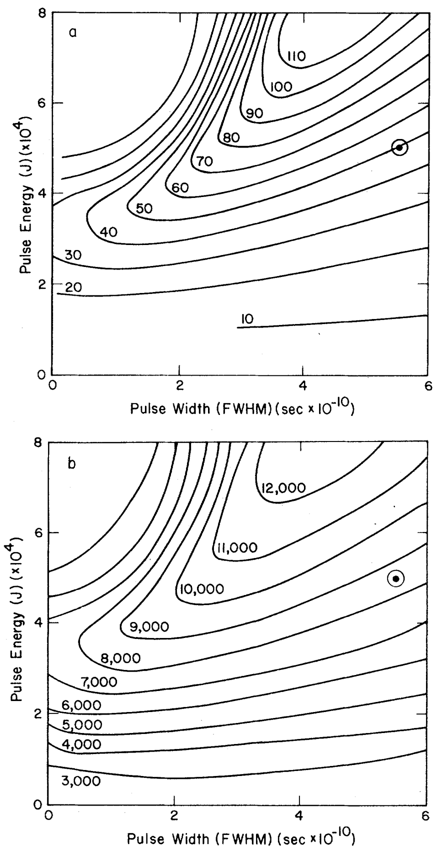

FIG. 1. Contours of (a) maximum center density in g/cm^3 and (b) temperature in eV at time of maximum density as a function of pulse energy, E, and full width at half-maximum, τ. Circled points indicate the example case.

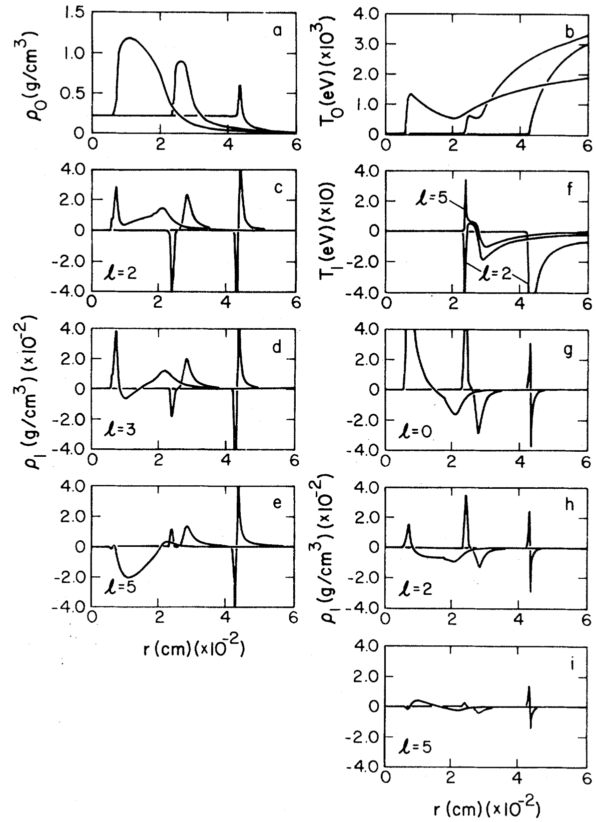

FIG. 2. Zero- and first-order quantities as a function of r at times $t = -0.21\times10^{-9}$, $+0.24\times10^{-9}$, and $+0.53\times10^{-9}$ sec with respect to the peak of the Gaussian pulse.

sen here as our example was taken from a study of implosions of 500-μm-radius frozen DT spheres isotropically irradiated by Gaussian laser pulses with a wavelength of 1.06 μm. The zero-order computations were done by a single-temperature Lagrangian hydrodynamics code with electron thermal conduction. Figure 1(a) is a contour plot of the maximum central densities achieved as a function of the total pulse energy, E, and the full width of the pulse at half-maximum, τ. Figure 1(b) is a plot of the corresponding center temperatures at the times of maximum density. The circled points indicate the case chosen, $E = 50$ kJ, $t = 5.5\times10^{-10}$ sec. This case, which is on the long-pulse side of that value of τ which gives the maximum density for the chosen value of E, produces a shock clearly separated from the ablation surface and a shocked region in between that is much cooler than the blowoff plasma during most of the implosion. In Figs. 2(a) and 2(b) the zero-order density and temperature, ρ_0 and T_0, are plotted at three different times ($t = -0.21\times10^{-9}$, $+0.24\times10^{-9}$, and $+0.53\times10^{-9}$ sec) with respect to the peak time of the Gaussian pulse, on the same axes. As we go out from $r=0$, the shock is where ρ_0 and T_0 rise sharply; the ablation front is where ρ_0 subsequently falls sharply just outside its maximum and T_0 begins to rise again. This class of implosion is quite similar to those produced by highly optimized pulses up to a time just before peak compression (see Refs. 2 and 3 for further references). Values of τ near the maximum density value or on the short-pulse side give implosions in which the ablation and shock surfaces are not so clearly separated, the region just behind the shock is not very much cooler than the blowoff plasma, and the resulting higher themal conductivity in this region further increases the stability of the flow. It is not asserted that this case is the least-stable possible case but rather that this case is representative of those relevant to laser fusion. *We do not know of a relevant* *class of homogeneous-pellet cases which we expect would be significantly less stable.*

Angle-dependent first-order perturbations of all zero-order dependent variables are represented by time- and radius-dependent coefficients of spherical harmonics of various l values, and are calculated by integration along the unperturbed characteristics of the zero-order Lagrangian flow, according to the method described in Ref. 2. Ablation stability is isolated from effects of illumination asymmetry by the assumptions of symmetric irradiation and an initial perturbation of the pellet of the incompressible form

$$\xi_r = \xi_0(r/a)^{l-1},$$
$$(\nabla\cdot\vec{\xi})_{\bar{\Omega}} = -(l+1)(\xi_0/a)(r/a)^{l-2},$$

which gives the pellet a bumpy surface. The unperturbed radius of the pellet is a, which is 500 μm for the case shown here. The scale of all first-order quantities is set by our taking $\xi_0 = 1$ μm, and thus giving the bumpy surface this amplitude. We prefer this form of regular initial perturbation over the random-noise approach of Shiau, Goldman, and Weng[3] for estimating the effect of initial pellet irregularities and any instability on implosion symmetry. Figures 2(c)–2(e) show the perturbed density coefficients ρ_1 for $l = 2$, 3, and 5, respectively, at the same three times at which ρ_0 and T_0 are plotted. At $t = -0.21 \times 10^{9}$ sec for all l's, the inside negative spike of ρ_1, which is well resolved by our grid, comes mostly from the convective contribution given by the product of the large $\partial\rho_0/\partial r$ at the shock and $-\xi_r$ there. The negative sign of the spike reflects the fact that at the angular phase $\cos\theta = 1$, where first-order quantities are defined, and, in general, wherever $Y_l^m(\bar{\Omega}) > 1$, the perturbed surface is initially raised, i.e., displaced outward, and the inward progress of the shock is retarded at early times relative to the zero-order flow by having to pass through additional material. The outward displacement of the critical surface, in the vicinity of where the light is absorbed, also contributes to shock retardation at this angular phase. Artificial viscosity distributes the shock jump, which is in principle discontinuous, over enough zones to permit accurate calculation of ρ_1 and other first-order quantities. The area under this spike is a measure of the perturbed radial shock displacement. The rest of ρ_1 behind the shock can be taken at face value. The positive feature of ρ_1 at $t = -0.21 \times 10^{-9}$ sec for all l's is also primarily convective, reflecting the initial outward displacement and the negative $\partial\rho_0/\partial r$ of the ablation front.

Subsequently, the following sequence of events occurs for all $l > 1$. Angular thermal conductivity increases the total heat flow into the regions of $\bar{\Omega}$ in which the surface of the pellet is initially raised, causing material to be ablated from these regions with greater energy, i.e., with greater specific impulse. The greater ablation pressure in the initial raised regions of $\bar{\Omega}$ causes the shock to be stronger there and hence to produce a higher shocked pressure behind and to move inward faster. The shock in the initially depressed regions of $\bar{\Omega}$ is correspondingly weaker and slower than the zero-order shock. The shock in the raised regions, which starts out retarded, in fact catches up with and moves ahead of the zero-order shock. This is first seen for $l = 5$ in Fig. 2(e) at $t = 0.24 \times 10^{-9}$ sec from the sign reversal of the spike in ρ_1 at the shock front from negative at the earlier time to positive. The same transition is seen to occur between $t = 0.24 \times 10^{-9}$ and 0.53×10^{-9} sec for $l = 2$ and 3. This motion of the shock front from one side of its zero-order position to the other might be expected to exhibit overstability, but this has not been observed. Thus, the observed behavior is positively stable. The reversal of shock retardation occurs sooner at higher l numbers because the angular wavelength is shorter and the angular thermal conduction is larger, as discussed in detail in Ref. 2.

The angular variation of perturbed pressure behind the shock front also causes a perturbed angular fluid flow which decreases the density in the initially raised regions of $\bar{\Omega}$. This density decrease is seen in a fully developed state at $t = 0.53 \times 10^{-9}$ sec for $l = 5$ and it is beginning to occur for $l = 3$. The above behavior corresponds to a tendency for the implosion to converge to separate points located on those radii on which there occurred initial minima of the pellet surface radius, i.e., minima of $Y_l^m(\bar{\Omega})$, as opposed to converging uniformly to the spherical center. This tendency to form local density maxima in the imploding shell of compressed material can be seen from the fact that Fig. 2(e) at $t = 0.53 \times 10^{-9}$ sec exhibits a negative maximum of ρ_1 at the same radius as the maximum of ρ_0 [Fig. 2(a)]. (If, on the other hand, the maximum of ρ_1 occurred in either of the regions of large $\pm\,\partial\rho_0/\partial r$ and if the zeros of ρ_1 and $\partial\rho_0/\partial r$ coincided, it would instead indicate only a waviness of the surface of maximum density with no isolated points of maximum density on this surface.) Figure 2(f) helps in visualizing the ablation stabilization process described above. On the same scales are plotted T_1 for $l=2$ at $t=0.21\times10^{-9}$ sec and T_1 for $l=2$ and 5 at $t=0.24\times10^{-9}$ sec. The major contribution to $T_1(l=2,\ t=-0.21\times10^{-9})$ is from retardation of the nonlinear thermal wave form of T_0 [Fig. 2(b)] at this time. [T_1 for $l=3$ and 5 at this time is almost identical to $T_1(l=2)$]. However, between $t=-0.21\times10^{-9}$ and $+0.24\times10^{-9}$ sec the angular conduction damping of T_1 in the vicinity of the ablation front is significantly greater for higher l's. Thus, at $t=0.24\times10^{-9}$ sec in this vicinity the negative magnitude of $T_1(l=5)$ is noticeably smaller than that of $T_1(l=2)$. However, in the shocked layer, where T_1 for $l=2$ and 5 is positive and almost flat, the magnitude of $T_1(l=5)$ is the greater, indicating stronger shocking as described above. The spikelike features nearest the origin are indicators of the perturbed shock displacement, just as are the corresponding ρ_1 features, and have opposite signs at this time because the $l=5$ shock has crossed over and $l=2$ has not. $T_1(l=3,\ t=0.24\times10^{-9})$ lies everywhere between $T_1(l=2)$ and $T_1(l=5)$. Inspection of $(\nabla\cdot\vec{\xi})_{\bar{\Omega}}$ shows that the additional curvature of the surface introduced by the surface perturbation also contributes to strengthening the shock and speeding the implosion in the initially raised regions of $\bar{\Omega}$ by making the implosion at early times converge more rapidly than in zero order, as if converging to points out from the origin on radii passing through initial maxima of $Y_l^m(\bar{\Omega})$. This purely hydrodynamic effect may make an important contribution to increasing the symmetry of imploding shells of fuel.

Regular initial perturbations of internal density give results very similar to those obtained from regular surface perturbations.

In order to learn the relative contributions of initial surface perturbations and of perturbations of illumination uniformity to implosion asymmetry, we have calculated the perturbed response of our same zero-order case to angular radiation variations scaled here to a relative modulation of 10^{-2}. Figures 2(g)–2(i) show the results for $l=0$, 2, and 5 at the same times as above. Comparison of such $l=0$ calculations with appropriately defined differences between two zero-order runs with only slightly different input power provides an extremely valuable verification of the numerical method. The $l=2$ and 5 results show the smoothing effect of higher l's pointed out in Ref. 2 although without the distinction made there between early- and late-time irradiation asymmetry. Comparison shows that for $l=2$ the magnitude of the late-time effect of an initial 1-μm surface-radius perturbation amplitude on this 500-μm-radius pellet (0.2%) is approximately the the same as that caused by a 1% variation of illumination intensity.

Similar calculations of the effects of these kinds of perturbation (incompressible bumpiness, perturbed density, and asymmetric illumination) have been done with 50-μm pellets with qualitatively very similar results.

It is pointed out in Refs. 1 and 2 that several physical effects that are neglected here, including thermoelectrically generated magnetic fields, spoil the m degeneracy and l decoupling of our perturbation treatment.

In fact Tidman and Shanny have pointed out[4] that spontaneously generated magnetic fields, which would reduce thermal conductivity, may grow unstably. However, at present such fields are being neglected not just for simplicity but also because experimental evidence indicates anomalous collision frequencies of such a large magnitude that the magnetic fields would be almost entirely suppressed. The understanding of laser-driven implosion stability will, however, not be satisfactory until this point is cleared up.

---

*This work performed under the auspices of the U. S. Atomic Energy Commision.

[1]D. B. Henderson and R. L. Morse, Bull. Amer. Phys. Soc. 18, 684 (1973).

[2]R. L. Morse, Bull. Amer. Phys. Soc. 18, 1359(T) (1973); D. B. Henderson and R. L. Morse, Phys. Rev. Lett. 32, 355 (1973).

[3]J. N. Shiau and E. B. Goldman, Bull. Amer. Phys. Soc. 18, 1358 (1973); J. N. Shiau, E. B. Goldman, and C. I. Weng. Phys. Rev. Lett. 32, 352 (1973).

[4]D. A. Tidman and R. A. Shanny, "Field Generating Thermal Instability In Laser Heated Plasma" (to be published).